Polym. Bull. (2009) 63:865–881
DOI 10.1007/s00289-009-0130-3

Effect of NBR partitioning agent on the mechanical properties of PVC/NBR blends and investigation of phase morphology by atomic force microscopy

Simoni Maria Gheno · F. R. Passador · L. A. Pessan

Received: 8 April 2009 / Revised: 10 June 2009 / Accepted: 29 June 2009 /
Published online: 19 July 2009

Abstract Poly(vinyl chloride) (PVC)/acrylonitrile–butadiene rubber (NBR) blends with different types of partitioning agent were obtained through melt blending. The samples were characterized according to the viscosities properties, torque rheometry and mechanical resistance as tensile testing, tear strength, and hardness. The morphology and phase imaging were studied using an atomic force microscopy operating in tapping mode (TMAFM). It was observed that the PVC/NBR blends with PVC as partitioning agent showed an increase in the tensile stress and Young's modulus compared to the PVC/NBR blends with calcium carbonate as partitioning agent. The morphology of the blends examined by TMAFM evidenced the effect of the partitioning agent as obtained with other techniques.

Keywords Poly(vinyl chloride) · Acrylonitrile–butadiene rubber · PVC/NBR · Blends · Imaging phase · AFM

Introduction

Polymers can be structured according to technological advances due to easiness of chemical modifications which can lead to the development of new materials with specific characteristics. However, their surface heterogeneity can affect their adhesion, wetting, and abrasion properties as well as the protection against

S. M. Gheno (✉) · F. R. Passador
PPGCEM, Federal University of Sao Carlos, Rod. Washington Luiz, km 235, P.O. Box 676, Sao Carlos, SP 13565-905, Brazil
e-mail: gheno@dema.ufscar.br

L. A. Pessan
Department of Materials Engineering, Federal University of Sao Carlos, Rod. Washington Luiz, km 235, P.O. Box 676, Sao Carlos, SP 13565-905, Brazil

environmental degradation. Therefore, identification and mapping of the surface are of great importance in science and technology.

PVC has been widely used in construction, transportation, and many other industries due to its high stiffness, flame retardancy, chemical resistance, and low cost. However, disadvantages of rigid PVC, such as low notched impact strength and low heat resistance have restricted its application [1, 2]. Thus, a possible alternative is polymer blend materials with balanced physical and chemical properties which fit to several applications.

Polymer blends are mostly immiscible, and therefore they tend to phase-separate [3]. Efforts have been employed to find new miscible combinations [3–5] since miscibility is of great importance in the development of morphology of polymer blends [4]. PVC/NBR blends features are due to the presence of acrylonitrile–butadiene rubber. Recent studies have characterized NBR as a rubber based thermoplastic elastomer that can improve the toughness of PVC [6–11]. To improve the toughness of PVC, an appropriate morphology is formed when NBR is dispersed into continuous PVC matrix [10].

The PVC/NBR blends are miscible physical mixtures of commercial importance and have attracted great interest of both researchers and industries due to their low cost/benefit and the significant increase in the toughness of brittle polymers through the incorporation of a dispersed elastomeric phase [6–11].

Besides, the knowledge of the interaction parameter in PVC/NBR blends is very important to understand their behavior because the NBR can act as a permanent plasticizer for PVC. The presence of PVC improves aging resistance of the NBR since both PVC and NBR are polar polymers, and blending NBR with PVC increases compatibility. Acrylonitrile–butadiene rubbers used in mixture with PVC resin are usually supplied in powder. This kind of NBR has a partitioning agent (PVC resin, calcium carbonate or silica) that is added after the polymerization of the NBR to avoid the agglomeration in the particles during the transport and storage. Extensive studies about PVC/NBR blends were presented by Liu et al. [12–17]. They reported that both miscibility and interaction between phases as well as the dispersion of the rubber phase are very important parameters to a better understanding of the performance of polymer blends. The pseudo-network morphology promoted quantitative improvements in impact resistance.

The interactions in blends of poly (vinyl chloride) (PVC) and acrylonitrile–butadiene rubber (NBR) as a function of the blend composition and the acrylonitrile (AN) content of NBR was investigated by Sen and Mukherjee [18] using the inverse gas chromatography. The authors observed that the two polymers are fairly miscible and show increased miscibility with the increase in the AN content of NBR [18].

Many techniques are used in the study of surfaces and properties of polymer blends [1, 2, 4–11, 19–24]. Among these techniques, the atomic force microscopy (AFM) is an innovative tool that can provide simultaneously the mapping of the surface topography and the phase heterogeneity with resolution up to an atomic resolution is. The phase detection microscopy (PDM) experiments run to investigate the mapping of different components are an important technique and have been widely used in research, mainly in polymer science [25].

Phase imaging or PDM can be used to map variations of surface properties such as viscoelasticity and elasticity. Phase imaging refers to the monitoring of the phase lag between the signal that drives the cantilever oscillation and the cantilever oscillation output signal. The phase lag is very sensitive to variations in material properties and to produce phase contrast [21].

In TMAFM the cantilever-tip system is oscillated at a frequency at or close to the resonance. The sample is imaged while the feedback adjusts the tip-sample separation to keep the oscillation amplitude at a fixed value [26]. Extensive studies about the tip motion in dynamic AFM presented a detailed understanding of the tip's motion as a function of sample properties, geometry of tip, and tip-sample separation [27–36].

The TMAFM is an operational AFM mode which makes it possible to use changes in the phase angle between the excitation and the tip oscillation of the AFM cantilever probe to produce a second image, the phase image also called phase contrast image. The phase mapping occurs due to the cantilever oscillation during the tapping mode scan. Phase imaging goes beyond simple topographical mapping to detect variations in composition, adhesion, viscoelasticity, and perhaps other properties [20–24].

Efimov et al. [37] investigated the block face of the biological or polymer sample by AFM phase to understand the correspondence of the stained structures and their macromolecular/phase composition.

Magonov and Reneker [38] studied the applications of state-of-the-art atomic force microscopy methods to elucidate the surface and near-surface structure of microlayer polyethylene (PE). The authors concluded that the stiffness-related contrast of the phase images offers new possibilities for imaging multicomponent polymer samples. This is confirmed by the phase images of several polymer systems.

Pickering and Vancso [39] studied thin films of phase separated polystyrene-b-polyisoprene-b-polystyrene block. Based on the fact that polystyrene (PS) phase and amorphous polyisoprene (PI) matrix have very different intrinsic properties the authors utilized the tapping mode atomic force microscopy (TMAFM) to study the contrast in the material property. The authors observed that the PS regions showed a lower adhesion, and, in heterogeneous systems with components of different compliances and adhesion, this could result in the observed changes and reversals in contrast images.

Liu [40] studied the AFM phase imaging to characterize ethylene propylene rubber (EPR) particle dispersion in impact copolymers and verified that the image analysis based on phase images provided information on particle size and size distribution and has become an alternative analytical method of traditional TEM characterization for materials with different phases and polymer blends.

One of the purposes of this work was to investigate the effects of addition of different kinds of partitioning agent in NBR to avoid the agglomeration of its particles during transportation and storage in the morphology and mechanical properties of PVC/NBR blends. Another goal was to develop the application and use of the tapping mode technique (TMAFM) to obtain contrast formation which in polymer phase imaging is older than 15 years and was developed by Zhong et al. [41].

Experimental

Materials

The poly (vinyl chloride) (PVC) used was a suspension grade PVC resin (Norvic SP 1300HP, supplied by Braskem, Brazil) with $\bar{M}_w \approx 200,000$ g/mol (characterized by a K value of 71 ± 1). The plasticizer added to the system was an industrial grade 2-ethylhexyl phthalate (DOP), and the thermal stabilizer was an industrial grade of barium and zinc base. Two commercial grades of acrylonitrile–butadiene rubber (Thoran NP-3351 C (sample name: NBR PC) and Thoran NP-3351 P (sample name: NBR PP), supplied by Petroflex, Brazil) with different partitioning agents were used as received. The specifications of the acrylonitrile–butadiene rubbers are listed in Table 1.

Preparation of PVC and NBR compound

The PVC was dry blended with 60 parts per hundred rubber (phr) of DOP and 3 phr of a stabilizer following usual procedures with an intensive mixer at 120 °C. The viscosity and the viscosity ratio at the shear rates range both PVC compound and NBR used during the process were evaluated using an Instron Capillary Rheometer (model 4467), with $L/D = 20$ at 160 °C.

Preparation of blends

The PVC compound, pure NBR with different type of partitioning agent**,** and PVC/NBR blends at the ratios of 90/10, 80/20, and 70/30 wt% of NBR PP and NBR PC were produced by melt blending using an internal mixer (Haake rheometer, model Rheomix 600) operated at 160 °C with cam rotors at 60 rpm for 5 min. The PVC/NBR blends (90/10, 80/20 and 70/30 wt%) were designated as follows: (i) NBR PP samples: PVC/NBR10 PP, PVC/NBR20 PP, and PVC/NBR30 PP, respectively; (ii) NBR PP samples: PVC/NBR10 PC, PVC/NBR20 PC, and PVC/NBR30 PC, respectively.

Table 1 Characteristics specifications of the acrylonitrile–butadiene rubbers used in this study

Properties	Method	Thoran NP-3351 C	Thoran NP-3351 P
Sample name		NBR PC	NBR PP
Specification	–	Not crosslinked	Partially crosslinked
Bound acrylonitrile (%)[a]	ITL 10.007	33.0 ± 2.0	32.5 ± 1.5
Mooney viscosity (MML 1 + 4 @ 100 °C)[a]	ASTM D-1646	48.0 ± 5.0	50.0 ± 5.0
Type of partitioning agent	–	Calcium carbonate ($CaCO_3$)	Poly (vinyl chloride) (PVC)
Partitioning agent content (%)	ITL 10.390	10.0 ± 2.0	12.5 ± 2.5

[a] Based on the copolymer

Mechanical testing

For each compound studied, a sheet with about 2.0 mm thick was prepared by compression-molding at 160 °C for 4 min, and the samples were cut into different geometries according to the standard required for each analysis performed using a pneumatic cutter (Ceast). The main mechanical tests were done as follows: (i) tensile test: carried out in a MTS Universal Testing Machine (model Aliance RT/5) according to ASTM D 638. The speed of the cross-head was 500 mm/min. Five specimens were used and the median value was taken for each case; (ii) tear test: carried out according to the ASTM D 1004 using a MTS Universal Testing Machine (model Aliance RT/5) at a cross-head speed of 51 mm/min. Five specimens were used and the average value was calculated; (iii) hardness: measured according to ASTM D-2240 and expressed in Shore A units; (iv) compression set: conducted on type I cylindrical test pieces strained to 25% of their original thickness and aged in an oven of controlled ventilation at 100 °C for 70 h.

Atomic force microscopy experiments

Samples of the PVC/NBR blends were cryogenically cracked in liquid nitrogen to avoid any possibility of phase deformation. Simultaneously, tapping mode topography and phase images are viewed side-by-side in real time with a scan speed of 0.8 Hz. In phase imaging, the phase lag of the cantilever oscillation, relative to the signal sent to the cantilever's piezodriver, is simultaneously monitored by the Quadrex Module and recorded by the Nanoscope IIIa SPM controller (Digital Instruments/Veeco Metrology, Inc., Santa Barbara, CA). The free sample surface was imaged using a NSC15 (MikroMasch) tip radius <10 nm, average force constant was 45 N/m and resonance frequency between 265 and 400 kHz were used for imaging in TMAFM. Before the tip engages the sample, the phase of the free cantilever oscillation was adjusted. Variation of the tip-to-sample force can be achieved by changing the driving amplitude (Da) and the set-point amplitude (Asp). The tip-to-sample force parameters used in this study as follow: typical value of free amplitude (Ao) was 2.0 V and the amplitude setpoint was 2.0 V after the tuning. The amplitude setpoint can be altered between 1.0 and 1.8 V during the scanning. The typical driving amplitude of the NSC15 tip was 50 mV. We use the same tip to imaging of all TMAFM analysis. Imaging was carried out at room temperature.

Results and discussion

PVC, NBR compound, and blends

The analysis of the viscosities under the mixing conditions for both PVC and NBR are showed in Fig. 1. The PVC compound and the NBR showed pseudoplastic behavior and the viscosity decreases with the increase in the shear rate [23, 42].

The viscosities as a function of the shear rate, for both PVC/NBR PC and PVC/NBR PP blends, with different contents of NBR are shown in Fig. 2. According to

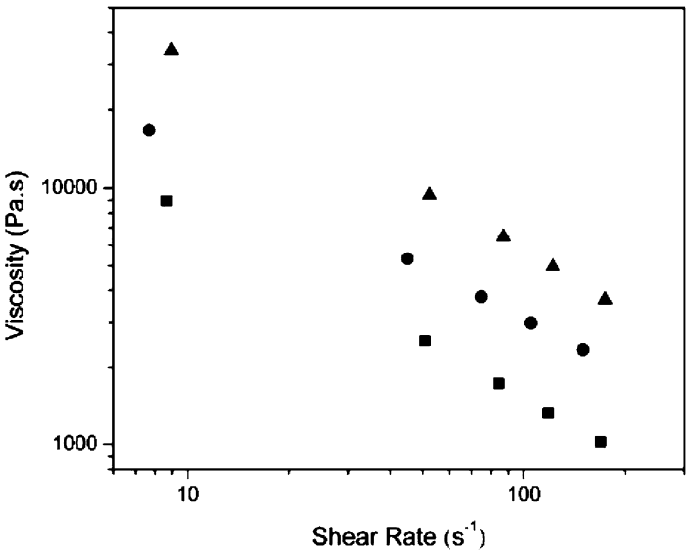

Fig. 1 Viscosity versus steady shear rate at 160 °C: PVC compound (*filled square*), NBR PC (*bullet*), and NBR PP (*filled triangle*)

the Taylor theory [43] of a Newtonian fluid dispersed in another Newtonian fluid under shear flow, when the viscosity ratios are between 0.7 and 3.7, the dispersed phase should extend into fibrils and break by capillary instability mechanisms (Tomokita theory) [43].

In this study, the blends were prepared in an internal mixer and the elongation at flow and coalescence phenomena should be taken into consideration since they are not considered in Taylor theory. Thus, it is expected that the morphology of PVC/NBR PC blends would be formed by a well-dispersed particulate phase of the NBR PC in the PVC matrix once the viscosity ratio is within the range estimated by Taylor. However, since the viscosity ratio between NBR PP and PVC composite is above the theoretical limit of 3.7, it is expected that the final morphology of PVC/NBR PP blends is composed of a dispersed phase of particulated shape. These results were reported in details by Passador et al. [2, 44].

The variation of torque and temperature during the mixing of PVC/NBR PC and PVC/NBR PP blends with different contents of NBR is shown in Fig. 3. It was observed that with the increase in mixing time, the torque also increases for both NBR PC and NBR PP. These results indicate that the partitioning agent interferes in the elastomer viscosity. NBR PP has high viscosity than NBR PC, as shown in Fig. 1. NBR PP is partially crosslinked, and during mixing the crosslinked particles of NBR contributes to increase in friction between the particles increasing the melt viscosity and consequently increasing the torque values of the blends. On the other hand, NBR PC is not crosslinked and showed a low viscosity compared to NBR PP and consequently a minor variation in the torque values with the increase of rubber

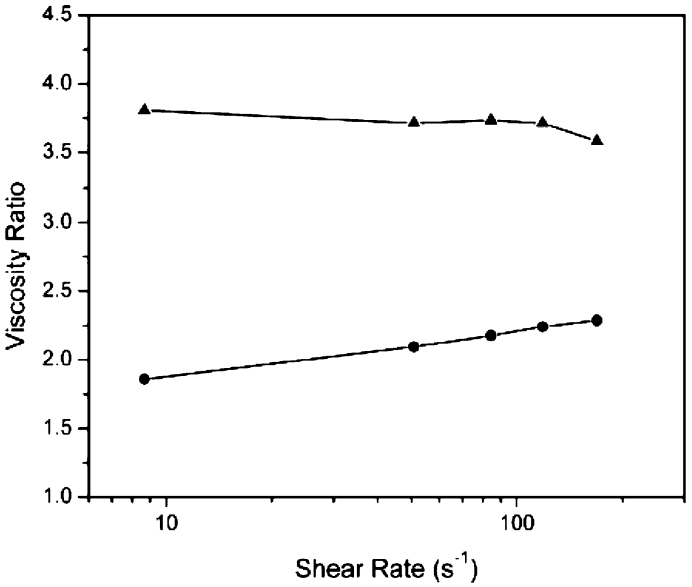

Fig. 2 Viscosity ratio versus steady shear rate at 160 °C of NBR PP/PVC compound (*-filled triangle-*) and NBR PC/PVC compound (*-bullet-*)

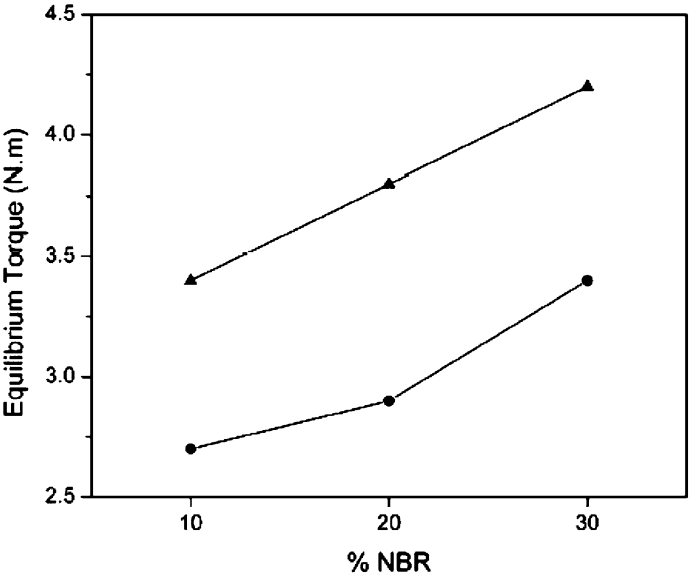

Fig. 3 Equilibrium torque versus NBR content of PVC/NBR PC (*-bullet-*) and PVC/NBR PP (*-filled triangle-*) blends

content. All blends showed that increasing the content of elastomer in the composition of the blend occurred increase in the equilibrium torque due the difference between the viscosities of the matrix and the dispersed phase.

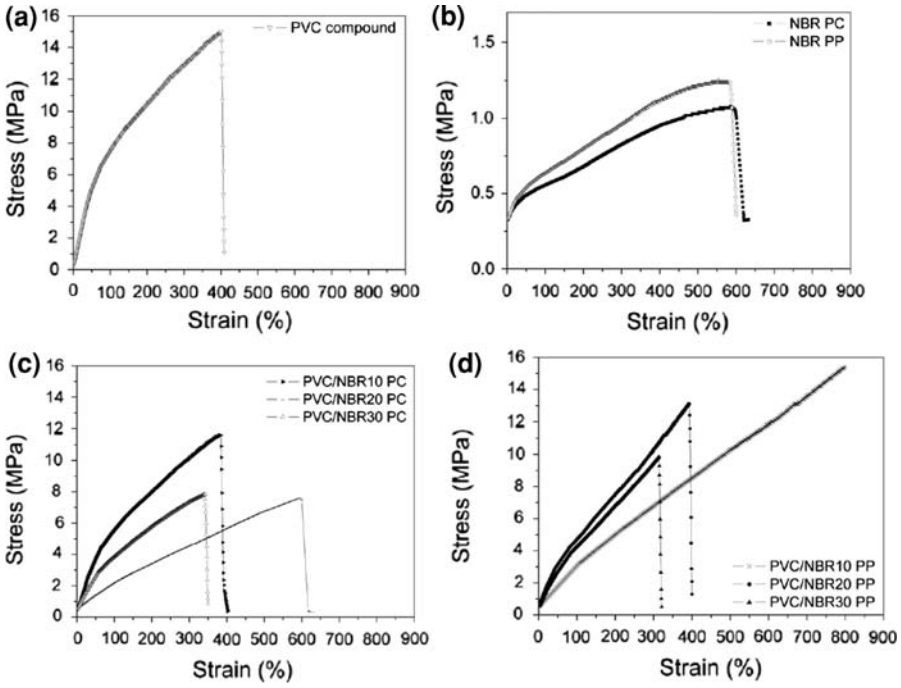

Fig. 4 Tensile stress–strain curves of the samples: (**a**) PVC compound, (**b**) NBR PC and NBR PP, (**c**) PVC/NBR10 PC, PVC/NBR20 PC and PVC/NBR30 PC, and (**d**) PVC/NBR10 PP, PVC/NBR20 PP and PVC/NBR30 PP

Mechanical testing

The mechanical strength of the PVC compound and NBR with different types of partitioning agents and the PVC/NBR PC and PVC/NBR PP blends were characterized by tensile testing, tear strength, hardness, and compression set.

Tensile tests

The tensile stress–strain curves of the samples are shown in Fig. 4. The calculated values of the tensile strength (σ_r), elongation at break (ε_r) and Young's modulus (E) are presented in Table 2.

The results of tensile strain showed that the NBR has low strength at break for NBR PC and NBR PP partitioning agents; however, NBR PP showed higher tensile at break than NBR PC. The addition of NBR in the PVC leads to blends with higher values of tensile strain compared to neat NBR. Another information refers to the tensile strain value which decreases with the increase of NBR content when compared to the value of the PVC compound. Blends of PVC/NBR PP showed higher tensile strain values. This behavior was expected because the NBR PP is partially crosslinked and NBP PC is not. Ehabe and Farid [45] also reported that the

Table 2 Mechanical properties of PVC compound, NBR and PVC/NBR blends

Sample	σ_r (MPa)	ε_r (%)	E (MPa)
PVC compound	15.2 ± 0.2	411.6 ± 11.6	10.55 ± 0.16
NBR PC	0.4 ± 0.1	605.8 ± 24.3	1.44 ± 0.13
NBR PP	0.9 ± 0.3	594.6 ± 15.7	1.36 ± 0.03
PVC/NBR10 PC	10.7 ± 0.4	406.3 ± 1.7	6.93 ± 0.17
PVC/NBR10 PP	14.7 ± 0.2	799.1 ± 19.6	2.61 ± 0.26
PVC/NBR20 PC	7.6 ± 0.1	595.4 ± 11.8	1.65 ± 0.05
PVC/NBR20 PP	12.5 ± 0.3	382.2 ± 12.6	6.29 ± 0.09
PVC/NBR30 PC	7.7 ± 0.2	347.3 ± 4.9	4.51 ± 0.10
PVC/NBR30 PP	11.1 ± 0.3	365.2 ± 11.5	5.17 ± 0.13

flexibility of rubber molecules enables blends to take up irregular and statistically random configurations.

The elongation at break results shows that the PVC compound has higher elongation at break due to the large amount of plasticizer used in its formulation, which favors the flexibility of the polymer chains [46]. No clear trend was observed in the elongation at break behavior of the blends with the increase of NBR content. The PVC/NBR PP blends have less elongation at break because the NBR PP is more rigid than the NBR PC. Some authors related this to the fact that elastomers have relatively low Young's modulus, which is in agreement with the results obtained in this study (Table 2) [7, 8]. As the NBR content in the blends increases, the Young's modulus decreases in comparison with the PVC compound. The Young's modulus for the PVC/NBR20 PC blend is lower than for the PVC/NBR30 PC. This behavior can be attributed to the dispersion of the elastomeric phase in the blend. In addition, it was verified that the highest values of Young's modulus are found for the blends that use NBR PP in their compositions.

Tear tests

Figure 5 shows the results of tear strength tests of the PVC compound, acrylonitrile–butadiene rubber, and blends. The results indicate that the increase in the NBR content leads to a decrease in the tear strength in the blends. This occurs because neat NBR has low tear strength in comparison to the PVC compound. The analysis of the effect of the partitioning agent in tear strength showed that PVC/NBR PP blends have higher tear strength than PVC/NBR PC blends once that the NBR PP contain reticulates in the polymer chains increasing the stiffness and tear resistance of this type of elastomers. The crosslinking formation increases the tear strength values especially for the composition with higher content of NBR, obtaining an increase of 240% in PVC/NBR30 PP blend compared with PVC/NBR30 PC.

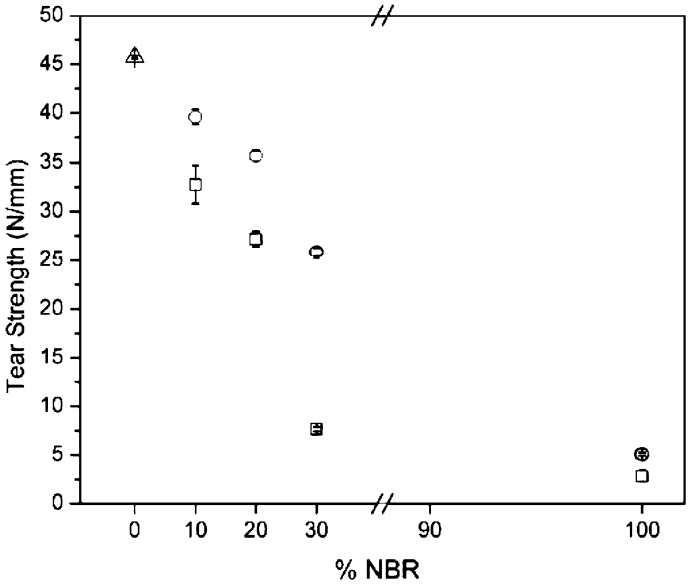

Fig. 5 Tear strength of PVC compound (*open triangle*), PVC/NBR PC blends (*open square*) and PVC/NBR PP blends (*open circle*)

Hardness tests

Figure 6 presents the hardness results of the PVC compound, NBR, and blends. The PVC compound presented higher hardness than NBR PC and NBR PP. Analyzing the blends hardness it can be observed that the increase in the acrylonitrile–butadiene rubber content in the blends composition reduces the hardness, if compared to the hardness of the PVC compound, due to low hardness of pure NBR. The influence of the partitioning agent on NBR showed that the PVC/NBR PP blends had superior hardness values than the PVC/NBR PC blends.

Compression set tests

Figure 7 presents the results of the compression set of the PVC compound, the acrylonitrile–butadiene rubber (NBR PP and NBR PC), and PVC/NBR blends with PVC and particulate $CaCO_3$ with 10, 20, and 30 wt% of NBR. The result shows that the highest resistance to compression is expressed in compression set terms. Figure 7 shows the NBR with different partitioning agents, and it can be seen that the NBR PC samples have a lower compression set value than PVC compound but are more resistant to compression when compared to NBR PP samples. It is worth mentioning that the PVC matrix has a high value of compression set which is expected due to its lower resistance to compression.

The type of partitioning agent used affects the behavior of blends compression set with the increase in the content of NBR in the compositions. In PVC/NBR PC blends, the increase in NBR level leads to a decrease in compression set values,

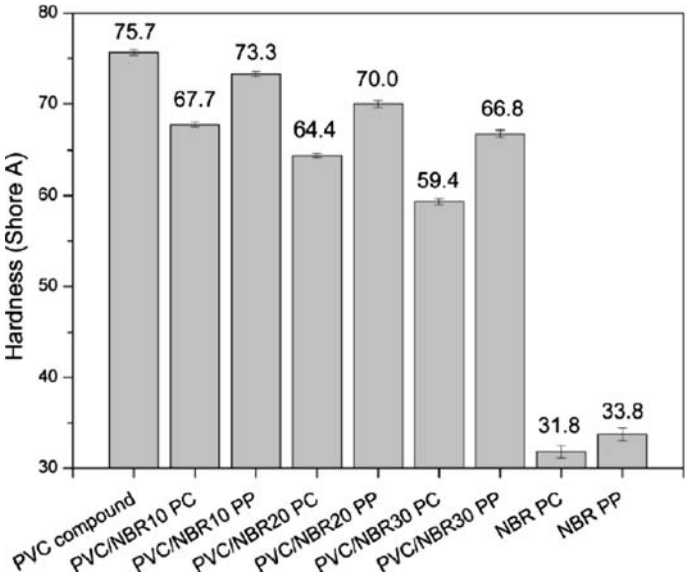

Fig. 6 Hardness values for the materials studied

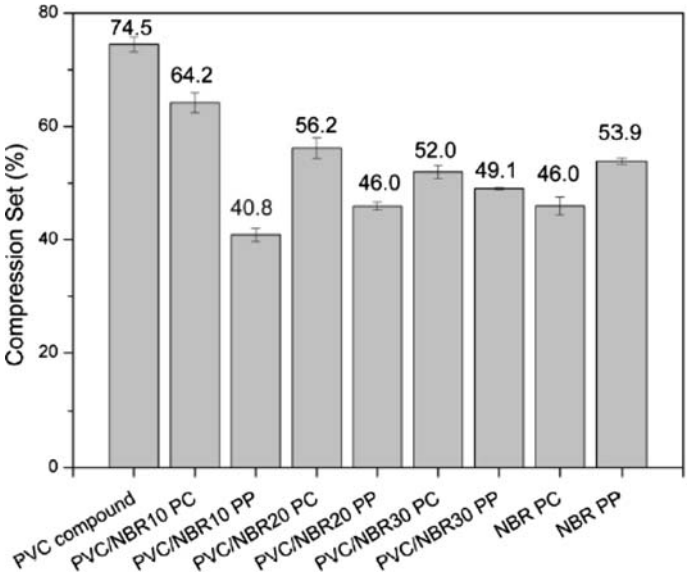

Fig. 7 Compression set values for the materials studied

i.e., an increase in the resistance to compression with increase in the NBR amount. The blends with PVC partitioning agent show a different behavior (Fig. 7); In these samples, the NBR amount increase led to an increase in the compression set value,

but theses values are lower than those of blends with $CaCO_3$ partitioning agent, and consequently they are considered more resistant to compression. The NBR PP is partially crosslinked and the increase of its amount in the blends leads to a significant increase in the compression set value caused by a movement restriction of elastomeric chains due to reticulation, which generates less elasticity of this phase, and consequently reduces the resistance to compression of the blends. Nevertheless, the PVC/NBR PP blends showed higher resistance to compression when compared with the PVC/NBR PC blends.

Atomic force microscopy

The surface and phase AFM imaging were used to characterize PVC/NBR samples (Figs. 8, 9). The images show dark and bright regions corresponding to the valleys and hills of the surface. The morphology observed in those images is important to identify the phase-separated regions and understand the phase contrast between these regions. Phase imaging was obtained simultaneously with tapping mode scan to detect variations in viscoelasticity and elasticity.

Figure 8 shows AFM images of PVC/NBR PC series. The surface images of PVC/NBR10 PC, PVC/NBR20 PC, and PVC/NBR30 PC, obtained by the tapping mode, are presented in Fig. 8a, c, and e, respectively. The phase images lead to the identification and mapping of different components in PVC/NBR samples through contrast difference. Figure 8b, d, and f shows a two-phase structure of the polymer blend clearly defined by the high resolution of phase imaging: the phase images highlights show the NBR PC phase, and the highlights and dark contrast in the phase image corresponds to low elasticity i.e., the PVC phase.

The morphology of PVC/NBR PC (Fig. 8b, d and e) shows spherical particles of the elastomer dispersed into the PVC matrix. It was observed that the increasing content of NBR in the blends leads to increase the particle size. This fact can be related to the particles coalescence phenomenon, possibly. The phase imaging of PVC/NBR PC (80/20) blend (Fig. 8d) showed that the elastomeric phase is agglomerated. This result can be to influence in blend stiffness, leading to high elongation at break (ε_r) and lower Young's modulus (E) than PVC/NBR PC (70/30) blend (Fig. 8f), as showed in Table 2.

Figure 9 shows AFM images of PVC/NBR PP series images. Figure 9a, c, and e shows the tapping mode images of PVC/NBR10 PP, PVC/NBR20 PP, and PVC/NBR30 PP, respectively. The phase imaging shows a two-phase structure of the polymer blend clearly defined by the high resolution of phase imaging: the phase images highlights show the NBR PP phase, and the dark contrast in the phase image corresponds to PVC phase.

The PVC/NBR PP blends (Fig. 9) showed the morphology of dispersed phase with spherical shape and small size particles. The results of the blends morphology with different partitioning agent indicate that the partitioning agent interferes significantly both the size and distribution of the elastomeric phase. Blends with the PVC partitioning agent showed the morphology of the elastomeric phase homogeneity dispersed with reduced particle size. The morphology development of the blends was affected by the kind of partitioning agent used in NBR (with

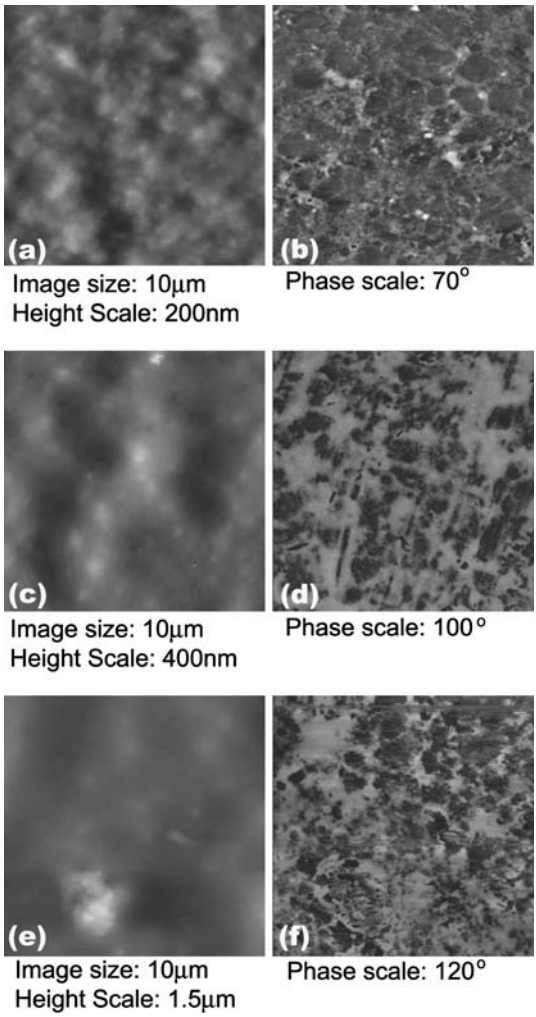

Fig. 8 Tapping mode images of PVC/NBR PC. PVC/NBR10 PC: topographic (**a**) and Phase shift (**b**); PVC/NBR20 PC: topographic (**c**) and Phase shift (**d**), and PVC/NBR30 PC: topographic (**e**) and phase shift (**f**). In **a**, **c**, and **e** it was observed that z-height is relation with NBR content. The phase image highlights shows PC phase

constant acrylonitrile content). This additive affects the rheological behavior of the PVC/NBR blends, increasing the viscosity ratio between NBR PP/PVC compound compared with NBR PC/PVC compound, and during the mixing the friction between the particles of NBR PP and PVC is higher compared with the friction between the particles of NBR PC and PVC. Also, the higher friction can be responsible for the decrease in particle size of the elastomeric phase and for the good dispersion of particles in the thermoplastic matrix. Thus, the combination of rheological behavior, processing conditions and the kind of partitioning agent contribute to the increase in mechanical strength of PVC/NBR PP blend, which associated with the crosslinked NBR lead to an increase of the rigidity of disperse phase, Young's modulus (E), hardness and tear strength when compared to those of blends with $CaCO_3$ partitioning agent which high particle size.

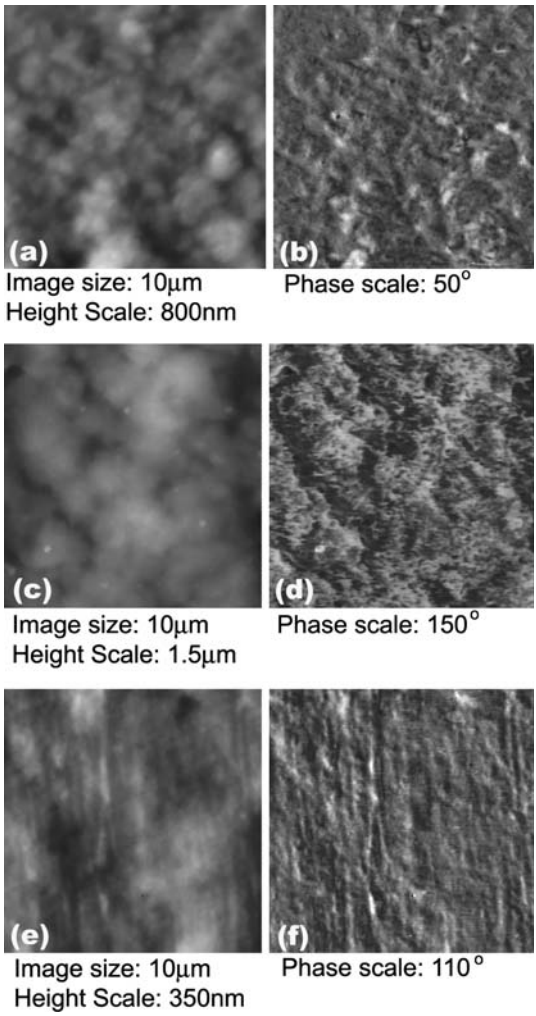

Fig. 9 Tapping mode images of PVC/NBR PP. PVC/NBR10 PP: topographic (**a**) and Phase shift (**b**); PVC/NBR20 PP: topographic (**c**) and Phase shift (**d**), and PVC/NBR30 PP: topographic (**e**) and Phase shift (**f**). In **a**, **c**, and **e** it was observed that z-height can relation with NBR content. The phase image highlights shows PP phase

The difference in the stiffness of the components at the sample surface can provide images with a phase contrast as observed in Figs. 8 and 9 indicate that the NBR PC and NBR PP polymer blends have higher elasticity than the PVC matrix in which they are embedded. These results indicate dispersion of the NBR components into the PVC matrix. The viscosity both the elastomer phase and PVC matrix are important factors that can be relation with phase imaging. The contrast obtained in the phase images is governed by many factors that affect tip-sample interactions including the mechanical properties and elastic inhomogeneity. The phase image provided strong contrast for NBR PC and NBR PP in the PVC matrix in detail. The size and shape of the phases vary with the NBR PC and NBR PP content in the sample.

Several theoretical studies which using the AFM technique are found in the literature and can be used to quantify the properties in polymers systems [1, 2, 4–11,

19–24, 27–40]. The phase imaging showed in Figs. 8 and 9 provide the best contrast of morphological features due to their high sensitivity TMAFM technique. These results are supported by study demonstrated by Efimov et al. [37], Magonov and Reneker [38], Pickering and Vancso [39], Liu [40].

As reported by Liu [40], for small interaction forces, the contrast is influenced by differences in adhesion force, as been observed in Figs. 8 and 9 to NBR PC and NBR PP and, PVC matrix. The adhesion would be expected to be much larger in the PVC/NBR PP blends than PVC/NBR PC.

Conclusions

The partitioning agent of acrylonitrile–butadiene rubber exerts great influence on the preparation process and on the mechanical properties of PVC/NBR blends. The mechanical properties results showed that the best performance of mechanical strength and hardness were obtained for the blends PVC/NBR PP, in which the partitioning agent is the PVC. These blends had better mechanical properties notably by higher values of tensile stress and Young's modulus compared to the PVC/NBR PC blends for different content of NBR analyzed.

The phase morphology of blends, analyzed by a powerful tool for mapping variations in sample properties at very high resolution, was greatly affected by the type of partitioning agent of the NBR. Phase imaging results clearly showed a two-phase structure of the polymer blend that was clearly defined by the phase imaging high resolution indicating that both PVC/NBR PC and PVC/NBR PP blends have higher elasticity than the PVC matrix in which they are embedded.

Acknowledgments The authors are grateful for the financial support provided by CAPES (Brazilian research supporting foundation), to Braskem S.A. for the donation of PVC, and to the technical support of the NEO-PVC Program.

References

1. Wang Q, Zhang X, Liu S, Gui H, Lai J, Liu Y, Gao J, Huang F, Song Z, Tan BH, Qiao J (2005) Ultrafine full-vulcanized powdered rubbers/PVC compounds with higher toughness and higher heat resistance. Polymer 46(24):10614–10617
2. Passador FR, Rodolfo A Jr, Pessan LA (2008) Influência do Tipo de Agente de Partição da Borracha Nitrílica na Obtenção de Blendas PVC/NBR. Polímeros, Ciência e Tecnologia 18(3):193–200
3. Utracki LA, Favis BD (1989) Polymer alloys and blends. In: Cheremisinoff NP (ed) Handbook of polymers science and technology. Hanser, Munich, pp 125–132
4. Corradini E, Rubira AF, Muniz EC (1997) Miscibility of PVC/EVA hydrolysed blends by viscosimetric, microscopic and thermal analysis. Eur Polym J 33(10–12):1651–1658
5. Painter PC, Graf JF, Coleman MM (1991) Effect of hydrogen bonding on the enthalpy of mixing and the composition dependence of the glass transition temperature in polymer blends. Macromolecules 24(20):5630–5638
6. George KE, Rani J, Francis DJ (1986) Studies on NBR/PVC blends. J Appl Polym Sci 32(1):2867–2873
7. Ismail H, Tan S, Poh BT (2001) Curing and mechanical properties of nitrile and natural rubber blends. J Elastom Plast 33(4):251–262

8. Mousa A, Ishiaku US, Ishak ZAM (2005) Oil resistance of dynamically vulcanized poly(vinyl chloride)/nitrile butadiene rubber thermoplastic elastomers. Polym Bull 53(3):203–212
9. Shen F, Li H, Wu CF (2006) Crosslinking induced by in situ coordination in acrylonitrile butadiene rubber/poly(vinyl chloride) alloy, filled with anhydrous copper sulfate particles. J Polym Sci: Part B: Polym Phys 44:378–386
10. Passador FR, Rodolfo A Jr, Pessan LA (2006) Estado de mistura e dispersão da fase borrachosa em blendas PVC/NBR. Polímeros, Ciência e Tecnologia 16(3):174–181
11. Passador FR, Rodolfo A Jr, Pessan LA (2007) Blendas PVC/NBR por processamento reativo I: Desenvolvimento do processo de vulcanização dinâmica in situ. Polímeros, Ciência e Tecnologia 17(2):80–84
12. Liu ZH, Zhu X, Wu L, Li RY, Qi Z, Choy C, Wang F (2001) Effects of interfacial adhesion on the rubber toughening of poly(vinyl chloride) Part 1. Impact tests. Polymer 42(2):737–746
13. Liu ZH, Wu LX, Kwok KW, Zhu XG, Qi ZN, Choy CL, Wan FS (2001) Effects of interfacial adhesion on the rubber toughening of poly(vinyl chloride) Part 2. Low-speed tensile tests. Polymer 42(4):1719–1724
14. Liu ZH, Zhang XD, Zhu XG, Qi ZN, Wang FS (1997) Effect of morphology on the brittle-ductile transition of polymer blends.1. A new equation for correlating morphological parameters. Polymer 38(21):5267–5273
15. Liu ZH, Zhang XD, Zhu XG, Li RKY, Qi ZN, Wang FS, Choy CL (1998) Effect of morphology on the brittle ductile transition of polymer blends: 2. Analysis on poly(vinyl chloride) nitrile rubber blends. Polymer 39(21):5019–5025
16. Liu ZH, Zhang XD, Zhu XG, Li RKY, Qi ZN, Wang FS, Choy CL (1998) Effect of morphology on the brittle ductile transition of polymer blends: 3. The influence of rubber particle spatial distribution on the fracture behaviour of poly(vinyl chloride)/nitrile rubber blends. Polymer 39(21):5027–5033
17. Liu ZH, Zhang XD, Zhu XG, Li KY, Qi ZN, Wang FS, Choy CL (1998) Effect of morphology on the brittle ductile transition of polymer blends: 4. Influence of the rubber particle spatial distribution in poly(vinyl chloride)/nitrile rubber blends. Polymer 39(21):5035–5045
18. Sen AK, Mukherjee GS (1993) Studies on the thermodynamic compatibility of blends of poly(vinylchloride) and nitrile rubber. Polymer 34(11):2386–2391
19. Hafezi M, Nouri Khorasani S, Ziaei F, Azim HR (2007) Comparison of physicomechanical properties of NBR–PVC blend cured by sulfur and electron beam. J Elastom Plast 39(2):151–163
20. San Paulo A, García R (2000) High-resolution imaging of antibodies by tapping-mode atomic force microscopy: attractive and repulsive tip-sample interaction regimes. Biophys J 78(3):1599–1605
21. Magonov SN, Elings V, Whangbo MH (1997) Phase imaging and stiffness in tapping-mode atomic-force microscopy. Surf Sci 375(2–3):L385–L391
22. Raghavan D, VanLandingham M, Gu X, Nguyen T (2000) Characterization of heterogeneous regions in polymer systems using tapping mode and force mode atomic force microscopy. Langmuir 16(24):9448–9459
23. Raghavan D, Gu X, Nguyen T, VanLandingham M, Karim A (2000) Mapping polymer heterogeneity by phase imaging and nanoindentation AFM. Macromolecules 33(7):2573–2583
24. Stark M, Möller C, Müller DJ, Guckenberger R (2001) From images to interactions: high-resolution phase imaging in tapping-mode atomic force microscopy. Biophys J 80(6):3009–3018
25. Garcia R, Calleja M, Pérez-Murano F (1998) Local oxidation of silicon surfaces by dynamic force microscopy: Nanofabrication and water bridge formation. Appl Phys Lett 72(18):2295–2297
26. Garcia R, San Paulo A (2000) Amplitude curves and operating regimes in dynamic atomic force microscopy. Ultramicroscopy 82:79–83
27. Tamayo J, Garcia R (1996) Deformation, contact time and phase contrast in tapping mode scanning force microscopy. Langmuir 12:4430–4435
28. Burham NA, Behrend OP, Ouveley F, Gremaud G, Gallo PJ, Gordon D, Dupas E, Kulik AJ, Pollock HM, Briggs GAD (1997) How does a tip tap? Nanotechnology 8:67
29. Garcia R, San Paulo A (1999) Attractive and repulsive tip-sample interaction regimes in tapping-mode atomic force microscopy. Phys Rev B 60(7):4961–4967
30. Garcia R, San Paulo A (2000) Dynamics of a vibrating tip near or in intermittent contact with a surface. Phys Rev B 61(20):13381–13384
31. Rodriguez TR, Garcia R (2002) Tip motion in amplitude modulation (tapping-mode) atomic-force microscopy: comparison between continuous and point-mass models. Appl Phys Lett 80(9):1646–1648
32. Garcia R, Perez R (2002) Dynamic atomic force microscopy methods. Surf Sci Report 47:197–301

33. Garcia R, San Paulo A (2002) Unifying theory of tapping-mode atomic-force microscopy. Phys Rev B 66:041406 (R)
34. Martinez NF, Garcia R (2006) Measuring phase shifts and energy dissipation with amplitude modulation atomic force microscopy. Nanotechnology 17:S167–S172
35. Martinez NF, Patil S, Lozano JR, Garcia R (2006) Enhanced compositional sensitivity in atomic force microscopy by the excitation of the first two flexural modes. Appl Phys Lett 89:153115b
36. Herruzo ET, Garcia R (2007) Frequency response of an atomic force microscope in liquids and air: magnetic versus acoustic excitation. Apll Phys Lett 91:143113
37. Efimov AE, Tonevitsky AG, Dittrich M, Matsko NB (2007) Atomic force microscope (AFM) combined with the ultramicrotome: a novel device for the serial section tomography and AFM/TEM complementary structural analysis of biological and polymer samples. J Microsc 226(3):207–217
38. Magonov SN, Reneker DH (1997) Characterization of polymer surfaces with atomic force microscopy. Annu Rev Mat Sci 27:175–222
39. Pickering JP, Vancso GJ (1998) Apparent contrast reversal in tapping mode atomic force microscope images on films of polystyrene-b-polyisoprene-b-polystyrene. Polym Bull 40:549–554
40. Liu J (2003) AFM applications in petrochemical polymers. Microsc Microanal 9(2):452–453
41. Zhong Q, Inniss D, Kjoller K, Elings V (1993) Fractured polymer/silica fiber surface studied by tapping mode atomic force microscopy. Surf Sci Lett 290:L688–L692
42. Schramn G (1994) A practical approach to rheology and rheometry, 2nd edn. Haake, Gebhard Schramm, Germany, pp 32–45
43. Utracki LA, Shi ZH (1992) Development of polymer blend morphology during compounding in a twin-screw extruder. I: Droplet dispersion and coalescence: a review. Polym Eng Sci 32(24):1824–1833
44. Passador FR, Rodolfo A Jr, Pessan LA (2008) Blendas PVC/NBR por processamento reativo II: Caracterização físico-mecânica e morfológica. Polímeros, Ciência e Tecnologia 18(2):87–91
45. Ehabe EE, Farid SA (2001) Chemical kinetics of vulcanisation and compression set. Euro Polym J 37(2):329–334
46. Rodolfo Jr. A, Nunes LR, Ormanji W (2006) Tecnologia do PVC. São Paulo: Proeditores/Braskem, p 365